OPTOELECTRONICS LETTERS Vol.9 No.4, 1 July 2013

An integrated optical 3D electric field sensing system based on time-division multiplexing

LI Wan-jun (李万军)*, **CHEN Fu-shen** (陈福深), **and ZHANG Jia-hong** (张家洪)
School of Communication and Information Engineering, University of Electronic Science and Technology of China, Chengdu 611731, China

(Received 11 March 2013)

A new integrated optical three-dimensional (3D) electric field (E-field) sensing system is shown in this paper. In the system, the method of tuning laser's wavelength is used for controlling the working point of the integrated optical E-field sensor to keep it always in linear working area. The sensing system contains three independent E-field sensors, and the tuning of their working points and the sensing of electric signal are completed by adopting time-division multiplexing (TDM) technique. Then, the theoretical analysis and simulation of the working mechanism of the E-field sensing system are done in this paper. The results show that the bandwidth of electric signal is directly related with the tuning time of working point, and also determines the working rate of the controlling system.

Document code: A **Article ID:** 1673-1905(2013)04-0270-4
DOI 10.1007/s11801-013-3043-1

The technology of using capacitance probe and various antennas for E-field measurement has been relatively mature, and its application is very wide[1]. But in the application, the sensors made by using electronic technology also have many shortcomings, and the most serious one is disturbing the E-field measurement[2]. In extra-high voltage or high power test, this kind of sensor probes containing lots of circuits are likely to be destroyed by the test field with high voltage[3]. At present, the integrated optical E-field sensors with the features of high sensitivity and high bandwidth[4] have been used for the electromagnetic compatibility testing (EMC)[5], intensive E-field pulse testing[6-8], humidity sensing[9], and especially for high voltage test with power frequency[10]. However, the drift of working point in the integrated optical device will affect the sensitivity and dynamic range of the sensor[11]. Now, most of integrated optical E-field sensors are one-dimensional, which can only sense a fixed direction of E-field or a field component[12]. There have been many researches about the traditional three-dimensional (3D) E-field sensors and systems[13,14], but the researches about integrated optical 3D E-field sensors and systems are still few. In this paper, an integrated optical 3D E-field sensing system based on time-division multiplexing (TDM) is designed and fabricated.

The integrated optical 3D E-field sensing system proposed in this paper is shown as Fig.1. In Fig.1, the antennas of three sensors are orthogonally arranged to form a rectangular coordinate system in 3D space. The E-field vector in any direction of space can be decomposed to three orthogonal components (along x, y and z directions) in this rectangular coordinate system. The three orthogonal E-field components are respectively parallel to the antennas of three sensors, so the output signals of three sensors represent the three components of E-field signal in the space.

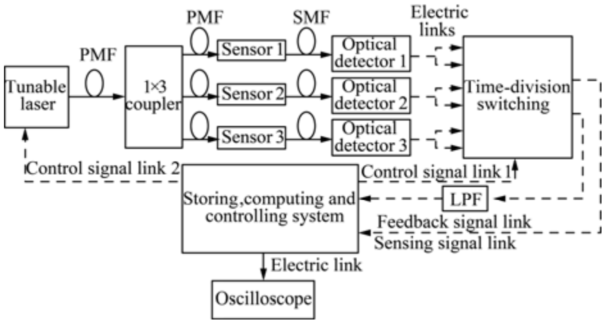

Fig.1 Integrated optical 3D E-field sensing system

The sensors in Fig.1 are fabricated based on lithium niobate material adopting Mach-Zehnder (M-Z) structure. And the transfer function of M-Z E-field sensor is described as follows[11]:

$$P_{\rm out}=\frac{1}{2}\alpha P_{\rm in}[1+\cos(\pi\frac{u(t)}{u_\pi}+\varphi)]\,, \tag{1}$$

where α is the loss factor of the system, $u(t)$ is the induced external electric signal on electrode or antenna, u_π is half-wave voltage, and φ is the biasing phase. In order to control the sensor's working point effectively, we choose a waveguide structure as shown in Fig.2. Through tuning the output light wavelength of the laser

---

* E-mail: liwanjun511322@163.com

in C waveband, we can find the proper one to achieve optical offset of the working point.

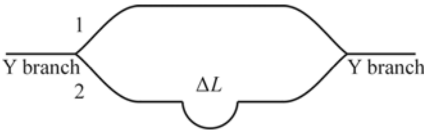

Fig.2 Schematic diagram of the asymmetric M-Z structure

Therefore, the system shown in Fig.1 adopts the TDM scheme to control the working points of three sensors.

It is deserved to be mentioned that sensor 1 is not only the tuning object but also the current worker of the sensing system. When the tuning of sensor 1 is completed, the sensing signal from SSL should be sampled by analog to digital converter (ADC), and then the sample data should be saved. The sensors 2 and 3 are handled in the same way. After a tuning cycle, SCCS can get an array containing three elements which respectively represent three orthogonal component values of the external E-field. So the real amplitude and vibrating direction can be easily calculated with the three orthogonal components. After that, the sampled signal is transmitted to an oscilloscope through the digital to analog converter (DAC) and low pass filter (LPF), and its waveform and phase information can be observed.

The expression of the external E-field can be described as:

$$\boldsymbol{E}(\boldsymbol{r},t)=\boldsymbol{r}\cos(\omega t+\theta_0)\,, \tag{2}$$

where $\boldsymbol{r}=E_0\boldsymbol{r}_0$ is the oscillatory direction vector of E-field, and E_0 is the maximum amplitude of E-field. $\boldsymbol{r}_0$ is the oscillatory direction unit vector of E-field and $\boldsymbol{r}_0=[\cos(\alpha),\cos(\beta),\cos(\gamma)]$, where α, β and γ are the included angles between the unit vector and rectangular coordinate axis x, y and z, respectively. ω is the oscillatory angular frequency of E-field, and θ_0 is the initial phase of E-field.

From Eq.(2), three components of the external E-field in axis x, y and z can be described as follows:

$$E_x(t)=E_0\cos(\alpha)\cos(\omega t+\theta_0)\,, \tag{3}$$

$$E_y(t)=E_0\cos(\beta)\cos(\omega t+\theta_0)\,, \tag{4}$$

$$E_z(t)=E_0\cos(\gamma)\cos(\omega t+\theta_0)\,. \tag{5}$$

If three sensors are working in linear area, set $\varphi=\pi/2$ and put Eqs.(3)–(5) into Eq.(2):

$$P_x(t)=\frac{1}{6}\alpha_x P_{\mathrm{in}}[1-\sin(\pi\frac{E_x(t)}{E_\pi})]\,, \tag{6}$$

where E_π is the half-wave E-field intensity of sensor, and it is assumed that half-wave E-field intensities of the three sensors are the same. Constant coefficient is 1/6, because the power is divided into three parts into three sensors. If $E_x(t)<<E_\pi$,

$$P_x(t)=\frac{1}{6}\alpha_x P_{\mathrm{in}}[1-\frac{\pi}{E_\pi}E_x(t)]\,, \tag{7}$$

and the same as direction x,

$$P_y(t)=\frac{1}{6}\alpha_y P_{\mathrm{in}}[1-\frac{\pi}{E_\pi}E_y(t)]\,, \tag{8}$$

$$P_z(t)=\frac{1}{6}\alpha_z P_{\mathrm{in}}[1-\frac{\pi}{E_\pi}E_z(t)]\,. \tag{9}$$

The output voltages of sensing signals through optical detector in axis x, y and z can be described respectively as:

$$V_x(t)=\frac{\eta e}{hf_{\mathrm{c}}}G\cdot\frac{1}{6}\alpha_x P_{\mathrm{in}}[1-\frac{\pi}{E_\pi}E_x(t)]\,, \tag{10}$$

$$V_y(t)=\frac{\eta e}{hf_{\mathrm{c}}}G\cdot\frac{1}{6}\alpha_y P_{\mathrm{in}}[1-\frac{\pi}{E_\pi}E_y(t)]\,, \tag{11}$$

$$V_z(t)=\frac{\eta e}{hf_{\mathrm{c}}}G\cdot\frac{1}{6}\alpha_z P_{\mathrm{in}}[1-\frac{\pi}{E_\pi}E_z(t)]\,, \tag{12}$$

where η is the photoelectric conversion efficiency, e is the electronic charge quantity, f_{c} is the oscillatory frequency of light wave, h is the Planck constant, and G is the gain of optical detector from current to voltage[15].

If working point tuning cycle of the single sensor is $T/3$, and the sampling period of sensing system is T, the sampled voltage signals are described as:

$$V_x(n)=V_x[1-\frac{\pi}{E_\pi}E_0\cos(\alpha)\cos(\omega Tn+\theta_0)],\quad n=0,1,2\cdots, \tag{13}$$

$$V_y(n)=V_y[1-\frac{\pi}{E_\pi}E_0\cos(\beta)\cos(\omega Tn+\theta_0)],\quad n=0,1,2\cdots, \tag{14}$$

$$V_z(n)=V_z[1-\frac{\pi}{E_\pi}E_0\cos(\gamma)\cos(\omega Tn+\theta_0)],\quad n=0,1,2\cdots, \tag{15}$$

where $V_x=\frac{\eta e}{hf_{\mathrm{c}}}G\cdot\frac{1}{6}\alpha_x P_{\mathrm{in}}$, $V_y=\frac{\eta e}{hf_{\mathrm{c}}}G\cdot\frac{1}{6}\alpha_y P_{\mathrm{in}}$ and $V_z=\frac{\eta e}{hf_{\mathrm{c}}}G\cdot\frac{1}{6}\alpha_z P_{\mathrm{in}}$.

From Eqs.(13)–(15), the direction angles of external E-filed can be calculated as:

$$\alpha(n)=\cos^{-1}[\frac{E_\pi}{\pi E_0\cos(\omega Tn+\theta_0)}(1-\frac{V_x(n)}{V_x})],\quad n=0,1,2\cdots, \tag{16}$$

$$\beta(n)=\cos^{-1}[\frac{E_\pi}{\pi E_0\cos(\omega Tn+\theta_0)}(1-\frac{V_y(n)}{V_y})],\quad n=0,1,2\cdots, \tag{17}$$

$$\gamma(n)=\cos^{-1}[\frac{E_\pi}{\pi E_0\cos(\omega Tn+\theta_0)}(1-\frac{V_z(n)}{V_z})],\quad n=0,1,2\cdots. \tag{18}$$

The amplitude of external E-field is calculated as：

$$E(n)=\frac{E_\pi}{\pi}r_0(n)V(n)E_0\cos(\omega Tn+\theta_0),$$
$$n=0,1,2\cdots, \tag{19}$$

where

$$r_0(n)=\sqrt{\cos^2(\alpha(n))+\cos^2(\beta(n))+\cos^2(\gamma(n))},$$
$$n=0,1,2\cdots, \tag{20}$$

$$V(n)=\sqrt{(1-\frac{V_x(n)}{V_x})^2+(1-\frac{V_y(n)}{V_y})^2+(1-\frac{V_z(n)}{V_z})^2},$$
$$n=0,1,2\cdots. \tag{21}$$

The vectorial expression of external E-field can be described as:

$$\boldsymbol{E}(n)=\frac{E_\pi}{\pi}\boldsymbol{r}_0(n)V(n)E_0\cos(\omega Tn+\theta_0), n=0,1,2\cdots, \tag{22}$$

$$\boldsymbol{r}_0(n)=[\cos(\alpha(n)),\cos(\beta(n)),\cos(\gamma(n))],$$
$$n=0,1,2\cdots. \tag{23}$$

According to the Nyquist sampling theorem, the original external E-field signal can be recovered with no distortion by letting the sampled signal through an appropriate LPF when $T<\pi/\omega$.

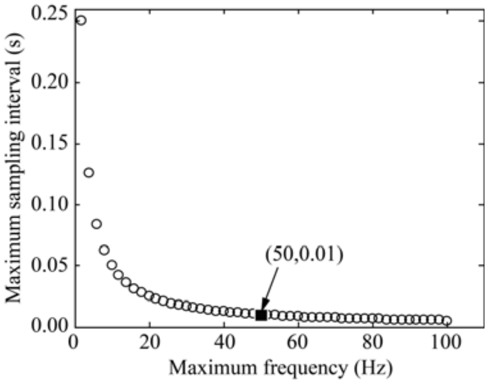

Fig.3 The relationship between maximum sampling interval and maximum signal frequency

From Fig.3, it is known that the tuning time of single sensor can be shorter with the increase of the highest frequency of signal. For the frequency point of 50 Hz, it is required that the tuning of single sensor must be completed in 0.01 s. If the maximum frequency increases further, there will be higher requirements for the tuning time of lasers, the time of sampling, calculating and controlling, and the switching time of TDS.

Taking the power frequency of 50 Hz as an example, it is assumed that the sampling time of the sensing system is 1 ms, and vibration direction vector is (cos(60°), cos(80°), cos(31.948°)), then the original signal and sampled signal are shown in Fig.4.

The changes of signal spectra before and after sampling are shown in Fig.5, and the spectrum of original signal is shown in Fig.5(a). The signal is a single frequency signal, so there are signals only at the frequency points of ±50 Hz. At this time, the spectrum of each signal component will become a periodic one with the period of 1 kHz. If let the three signal components through an appropriate LPF to eliminate the signal with frequency of more than 500 Hz and only reserve the signal near zero frequency, the original analog signal will be restored almost with no distortion. By using the sampling values of three signal components, the real signal amplitude and vibration direction vector of the external E-field can be calculated easily so as to realize the function of E-field sensing.

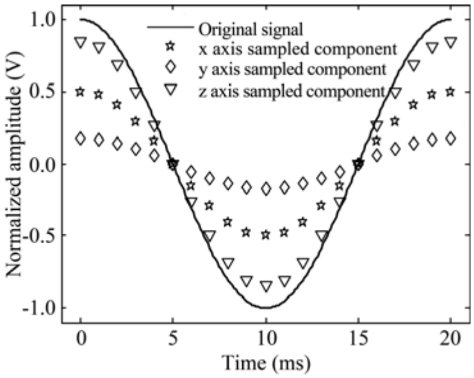

Fig.4 The original signal and sampled signal with sampling time of 1 ms and vibration direction vector of (cos(60°), cos(80°), cos(31.948°))

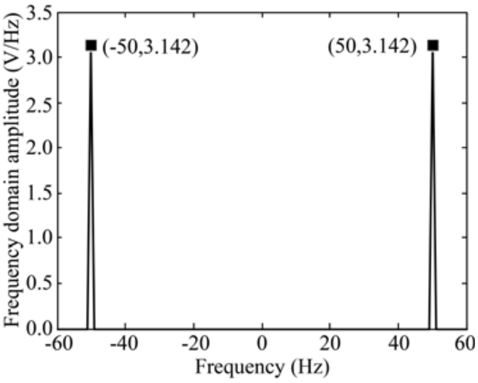

(a)

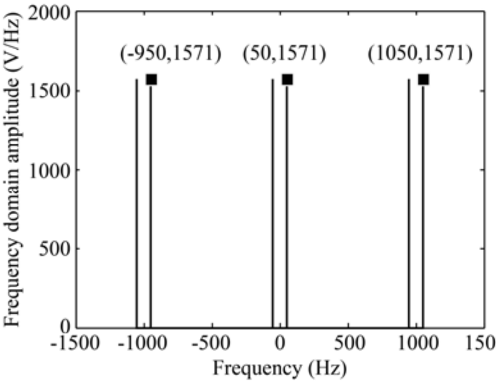

(b)

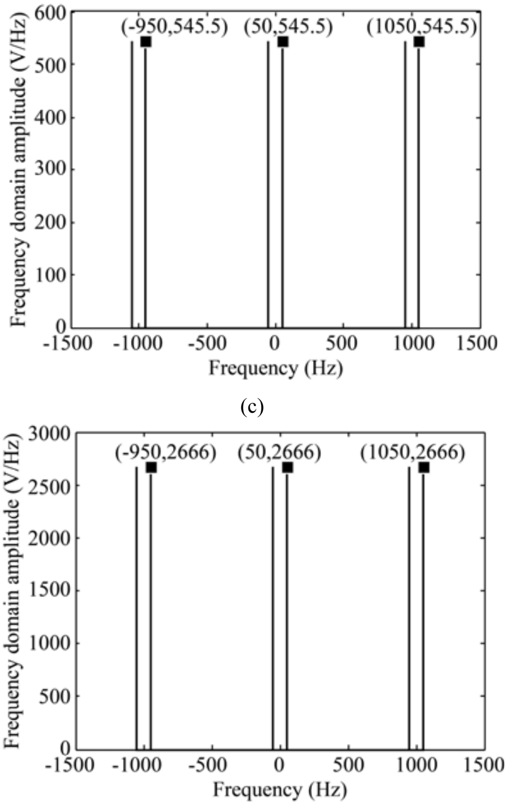

(c)

(d)

Fig.5 The spectra of (a) original signal and sampled signals in (b) *x*, (c) *y* and (d) *z* directions

This paper puts forward a new type of 3D integrated optical E-field sensing system based on TDM, and it realizes the automatic tuning of working points in three independent integrated optical E-field sensors. The sensing of E-field signal and the control of working points of sensors are synchronously completed. Compared with one or two dimensional E-field sensing systems, the 3D E-field sensing system can give a comprehensive and accurate sensing to the vibration direction, amplitude and phase of the E-field in space. This system uses a single optical source to control the working points of multiple sensors to reduce the cost. According to the theoretical analyses, it is known that the bandwidth of the signal is directly related to the working point tuning time of the sensing system, and at the same time it also determines the working rate of the controlling system.

References

[1] Wu Peng, Guo Xiao-fei, Chen Zhi-gao, Xia Jie-ning and Yang Jian, Journal of Geodesy and Geodynamics **32**, 141 (2012). (in Chinese)

[2] Zhang Zhan-long, Hu Ping and Li Jing-xiong, Journal of Chongqing University **35**, 19 (2012). (in Chinese)

[3] Wang Yang-yang, Gao Yong-sheng and Wang Zhen-xing, Journal of Hebei University of Science and Technology **32**, 119 (2011). (in Chinese)

[4] Hu Zhe-feng, Chen Fu-sheng, Sun Bao and Chen Shi, Laser Technology **35**, 688 (2011). (in Chinese)

[5] Cao Yong-sheng, Chen Fu-shen, Sun Bao and Gao Jie, Safety & EMC **4**, 20 (2012). (in Chinese)

[6] Wang Feng, Zeng Rong, Geng Yi-nan, Wang Bo and Niu Ben, Measurement of Lightning Impulse Electric Field Rod-plate Air Gap, High Voltage Engineering **37**, 2971 (2011). (in Chinese)

[7] Meng Qing-ying, Ren Guang-jun, Li Jing-hui and Yao Jian-quan, Journal of Optoelectronics·Laser **23**, 1713 (2012). (in Chinese)

[8] Qu Xin, Journal of Optoelectronics·Laser **22**, 163 (2011). (in Chinese)

[9] Yang Hui-qi, Lu Dan-feng and Qi Zhi-mei, Journal of Optoelectronics· Laser **22**, 1479 (2011). (in Chinese)

[10] R. Zeng, B. Wang, Q. Yu and W. Chen, IEEE Trans. Dielectr. Electr. Insul. **18**, 312 (2011).

[11] Sun Bao and Chen Fu-shen, Semiconductor Optoelectronics **30**, 672 (2009). (in Chinese)

[12] Si Rong-ren, Shi Li-hua, Chen Rui and Li Yan-xin, High Power Laser and Particle Beams **24**, 2930 (2012). (in Chinese)

[13] Xiang Ying-meng, Zhang Bin-rong, Wei Yu and Zhang Zhan-long, Journal of Chongqing University of Science and Technology **12**, 131 (2010). (in Chinese)

[14] Zheng Feng-jie and Xia Shan-hong, Journal of Electronics & Information Technology **34**, 1637 (2012). (in Chinese)

[15] Sun Bao and Chen Fu-shen, Chinese Physics Letters **26**, 024212-1 (2009).